THE JOURNAL OF GENE MEDICINE
J Gene Med 2011;**13:** 46–59.
Published online 8 December 2010 in Wiley Online Library (wileyonlinelibrary.com) **DOI:** 10.1002/jgm.1526

RESEARCH ARTICLE

Improved transfection efficiency of an aliphatic lipid substituted 2 kDa polyethylenimine is attributed to enhanced nuclear association and uptake in rat bone marrow stromal cell

Charlie Yu Ming Hsu[1]
Michael Hendzel[2]
Hasan Uludağ[1,3,4]*

[1]*Department of Biomedical Engineering, Faculty of Medicine and Dentistry, University of Alberta, Edmonton, Alberta, Canada*

[2]*Department of Oncology, Faculty of Medicine and Dentistry, University of Alberta, Edmonton, Alberta, Canada*

[3]*Department of Chemical and Materials Engineering, Faculty of Engineering, University of Alberta, Edmonton, Alberta, Canada*

[4]*Faculty of Pharmacy & Pharmaceutical Sciences, University of Alberta, Edmonton, Alberta, Canada*

*Correspondence to:
Hasan Uludağ, Department of Chemical and Materials Engineering, Faculty of Engineering, University of Alberta, Edmonton, Alberta, T6G 2G6 Canada
E-mail: hasan.uludag@ualberta.ca

Received : 27 September 2010
Revised: 3 November 2010
Accepted: 5 November 2010

Abstract

Background Lipid substitutions of cationic polymers are actively explored to enhance the efficiency of nonviral gene carriers. We recently took this approach to develop a novel gene carrier by grafting linoleic acid (LA) to relatively biocompatible 2 kDa polyethylenimine (PEI2). The resulting polymer (PEI2LA) displayed improved transfection efficiency over the unmodified PEI2. The intracellular kinetics and distribution of the respective polyplexes were investigated in the present study to gain a better understanding of the role of lipid modification in intracellular trafficking of gene carriers.

Methods A Cy5-labeled plasmid DNA (pDNA) expressing the green fluorescent protein (GFP) was complexed with PEI2, PEI2LA, and 25 kDa polyethylenimine (PEI25) to transfect rat bone marrow stromal cells (BMSC). Subcellular fractionation was performed to measure the amount of nuclear associated pDNA. pDNA uptake, GFP-expression and nuclear-associated pDNA were measured by both flow cytometry and confocal laser scanning microscopy.

Results PEI2LA mediated higher transgene expression and percentages of transfected cells than PEI25 and PEI2, respectively. There was a strong correlation between nuclear associated pDNA and transgene expression. PEI2LA polyplexes were significantly larger in size than PEI25. The amounts of pDNA associated with the nuclei were greater in PEI2LA than PEI25 polyplexes. The perinuclear pDNA distribution between GFP-expressing and nonGFP-expressing indicated that GFP-positive cells had a higher amount of pDNA associated with their nuclei.

Conclusions Improved transfection efficiency of PEI2LA was attributed to enhanced association with the nucleus, which may be a result of hydrophobic interaction between the lipid moieties on the modified lipopolymer and the nuclear membrane. Copyright © 2010 John Wiley & Sons, Ltd.

Keywords bone marrow; flow cytometry; gene transfer; nonviral vector; nuclear association; nuclei extraction

Introduction

Gene therapy is a promising therapeutic approach for a wide range of chronic and infectious diseases. The treatment is based on the accurate delivery of nucleic acids to the pertinent cells to correct the physiological abnormalities

at the genetic level. Successful gene therapy relies on the development of efficient gene carries to facilitate the entry of nucleic acid across the plasma membrane. Disarmed viral particles were initially employed for this purpose but mutagenic and immunogenic concerns prompted the development of safer alternative nonviral gene delivery systems [1]. Cationic polymers such as polyethylenimines (PEI) have been one of the most promising polymers for nonviral gene delivery as an alternative for viral vectors. The high density of cationic charges on PEI facilitates efficient binding to the anionic phosphate groups on nucleic acids, whereas the abundance of amine groups provides a suitable mean for further functionalization [2]. The latter feature allows various cell compatible ligands to be chemically conjugated to enhance the gene delivery efficiency of the carrier [3–8].

Among the ligands used to functionalize the cationic polymers, grafting lipid moieties such as cholesterol and aliphatic fatty acid to low molecular weight PEI has been shown to be an effective approach for improving the gene delivery and transfection efficiency of the polymer [9–11]. Our laboratory has pursued this approach to develop a novel water soluble amphiphatic polymer by grafting a series of aliphatic lipids (from C8 to C18) to a low molecular weight (2 kDa) PEI [12]. Among the lipids, the linoleic acid (LA) substitution was found to be particularly advantageous; the resulting polymer, PEI2LA, displayed significant improvement in transfection efficiency in the transformed human embryonic kidney cell line, HEK 293T, over the unmodified PEI2 [12]. Hydrophobic modification through lipid substitution may enhance polymer compatibility with cells by increasing affinity to lipid-based cellular membranes, such as the plasma membranes, thus promoting subsequent cellular uptake. This was shown to be the case with PEI2LA, where the degree of lipid substitution correlated directly with the uptake efficiency of the polyplexes [12].

Increased affinity to cellular membrane in lipid substituted polymers could also facilitate nuclear uptake of the DNA cargo through association with the nuclear envelope. The nuclear envelope acts as a physical barrier, separating the cytoplasm from the nucleoplasm. The double membrane structure permits passive entry of low molecular weight macromoleculess (<40 nm) [13], whereas larger molecules needs to be actively transported. Polyplexes with a size range of >100 nm are inherently too large to traverse through the nuclear pore complex embedded in the nuclear envelope and typically do not contain signal elements required to be actively imported. It has been suggested that entry may be opportunitistically permitted during mitosis when the nuclear envelope disintegrates [14–18]. That is, the transient removal of the membrane barrier during cell division allows plasmid DNA (pDNA) to be transported into the nucleoplasm. This form of 'nuclear uptake' would favor pDNA that are physically close to the nucleus before cell division. Thus, lipid-substituted polymer may increase nuclear uptake by maintaining the proximity of pDNA to the nucleus before cell division through polyplex association with the membrane. This issue has not been explored with previous lipid-substituted polymers.

A previous study was performed to screen a lipid-modified polymer library, which included PEI2LA polymers, aiming to identify effective pDNA carriers. Although PEI2LA appeared to be the best carrier to support transgene expression in HEK293T cells, little to no transfection was evident in bone marrow stromal cells (BMSC) in that preliminary study. Thus, PEI2LA was chosen for the present study to further explore transfection parameters and enhance its utility for gene delivery to BMSC. Furthermore, we aimed to characterize the intracellular distribution of the polyplex to gain a better understanding of the role of lipid substitution in cytoplasmic trafficking and nuclear routing. The pDNA was fluorescently labeled to track the amount of intracellular pDNA and the level of transgene expression simultaneously, which enabled us to directly correlate transfection efficiency with pDNA distribution. We further measured the amount of nuclear associated pDNA using both flow cytometry and confocal laser scanning microscopy (CLSM) to characterize the nuclear trafficking capability of PEI2LA in relation to its unmodified parental molecule PEI2, and branched 25 kDa polyethylenimine (PEI25). We demonstrate that PEI2LA displayed greater transfection efficiency over PEI2 via enhanced association with the nuclear periphery.

Materials and methods

Materials

The 2 kDa branched PEI (PEI2; $M_n = 1.8$ kDa, $M_w = 2.0$ kDa), 25 kDa branched PEI (PEI25; $M_n = 10$ kDa; $M_w = 25$ kDa), Hanks' balanced salt solution (HBSS, with phenol red) and trypsin/ethylenediaminetetraacetic acid (EDTA) were obtained from Sigma (St Louis, MO, USA). The PEI2LA was synthesized according to the synthetic scheme outlined previously [12], with a LA:PEI2 feed ratio of 0.1. The PEI2LA with an average substitution of 1.2 linoleic acids per polymer was obtained and used for these studies. Opti-MEM® I Reduced Serum Media, Dulbecco's modified Eagle's medium (DMEM; high and low glucose with L-glutamine), penicillin (10 000 U/ml) and streptomycin (10 mg/ml) were from Invitrogen (Grand Island, NY, USA). Fetal bovine serum (FBS) was from PAA Laboratories (Etobicoke, Ontario, Canada). The blank plasmid gWIZ (i.e. no functional gene product) and gWIZ-GFP (i.e. green fluorescent protein mammalian expression plasmid) were purchased from Aldevron (Fargo, ND, USA).

Plasmid labeling

The gWIZ-GFP plasmid is a 5757 bp mammalian expression plasmid which contains a modified promoter

DOI: 10.1002/jgm

from the human cytomegalovirus immediate early genes. gWIZ-GFP was labeled with the fluorophore Cy5 using the Label IT® Tracker™ Intracellular Nucleic Acid Localization Kit (Mirus Bio, WI, USA) in accordance with the manufacturer's instructions. Briefly, a 1:5 (v/w) ratio of dye to nucleic acid reaction mix was prepared and incubated at 37 °C for 1 h. Unbound and free Cy5 molecules were removed by ethanol precipitation after adding 0.1 volume of 5 M NaCl and two volumes of 100% ethanol. Purified labeled pDNA was then suspended in ddH_2O. Labeling efficiency was determined by calculating the ratio of base to dye using the equation $(A_{base} \times \varepsilon_{dye})/(A_{dye} \times \varepsilon_{base})$ by measuring absorbance at 260 nm (base) and 649 nm (dye) using the values $\varepsilon_{Cy5} = 250\,000$; $\varepsilon_{base} = 6600$ and $CF_{260} = 0.05$. The contribution of dye to the A_{260} reading was corrected by using the equation $A_{base} = A_{260} - (A_{dye} \times CF_{260})$. Plasmid DNA labeled using the concentration outlined yielded approximately 5 Cy5 labels per pDNA.

Cell culture and transfection

Rat bone marrow stromal cells (rBMSC) were isolated and cultured as described previously [19–20]. Briefly, cells were isolated from both femurs of 8-week-old female Sprague-Dawley rats and pooled to obtain a single suspension. The bone marrow was flushed out with 15 ml of DMEM containing 10% FBS, 50 μg/ml ascorbic acid, 100 U/ml penicillin and 100 μg/l of streptomycin (referred to hereon as basic medium). Cells were centrifuged for 6 min at 35 *g*, suspended in fresh basic medium and seeded in a single 75 cm^2 flask (Sarstedt; Montreal, QC, Canada). After medium change on day 3, the cells were trypsinized on day 7 and expanded in 75 cm^2 flasks (1:4 dilution). The rBMSC passaged between two and four generations were used in the present study, and were grown in multiwell plates for transfection studies.

Complex preparation

Self-assembled polymer/pDNA polyplexes were formed by first diluting the desired pDNA in 150 mM NaCl; cationic polymers were then added at a polymer-to-pDNA weight ratio of 5 (PEI25; N/P = ~38.7) or 10 (PEI2 and PEI2LA; N/P = ~75.5, assuming a similar MW for these two polymers), mixed using a vortex mixer and incubated at room temperature for 25 min. The polyplex solution were then diluted with nine volumes of OptiMEM (+1% FBS) to bring the final pDNA concentration to 3 μg/ml and incubated for an additional 20 min at room temperature. The diluted polyplex solutions were then added directly to the cells. For multiplexed flow cytometry and CLSM, labeled pDNA was mixed with unlabeled pDNA at a ratio of 1:2 before complexation.

Particle size measurement

The hydrodynamic size range of the polymer/pDNA complexes was measured by photon correlation spectroscopy (Zetasizer Nano, Malvern Instruments Ltd, Worcestershire, UK). Polyplexes were prepared at various polymer-to-pDNA weight ratios in 150 mM NaCl with a final volume of 100 μl and incubated for 25 min. The polyplex solutions were then diluted to 1 ml by adding 900 μl of OptiMEM (+1% FBS) to bring a final pDNA concentration of 2 μg/ml or a final polymer concentration of 10 μg/ml. Measurements were taken in a heated chamber set at 37 °C, at a wavelength of 660 nm and particle sizes were calculated by using a medium viscosity of 1.140 cP and a refractive index of 1.333 (at 37 °C). Values reported were an average of 12 measurements with 10-s interval between each measurement.

Polyplex uptake and transfection efficiency

The polyplexes were prepared as above and then added to rBMSC grown in six-well plates at a cell density of 70–80%. After a 4-h incubation with the polyplexes, the transfection medium (OptiMEM + 1% FBS) was replaced with the basic medium (DMEM + 10% FBS) and incubated at 37 °C until analysis. Processing for flow cytometry were done by first washing the cells twice with Ca^{2+}/Mg^{2+}-free (CMF) HBSS (without phenol red), then detached from tissue culture plates with 1 × Trypsin-EDTA (Gibco, Gaithersburg, MD, USA) and subsequently fixed in 3.7% formaldehyde in CMF-. Quantification of pDNA uptake and GFP expression were performed using a FACSCalibur (BD Biosciences, Franklin Lakes, NJ, USA); Cy5-labeled plasmid DNA uptake was measured in the FL4 channel using the red diode laser (633 nm); GFP fluorescence from the expression of the plasmid DNA was measured in the FL1 channel using the 488 nm blue laser. Analysis was performed by calibrating gating to the negative control (i.e. polymer complexes prepared with gWIZ) such that the autofluorescent cell population represented 1–2% of total cell population.

Nuclei isolation and quantification of nuclear-associated pDNA

To release nuclei from the cells, cells were detached from the tissue culture plates using 1 × Trypsin-EDTA as described above. Trypsin reaction was stopped by adding basic medium with 10% FBS. Cells were then pelleted by spinning at 150 ***g*** for 5 min, re-suspended in a hypotonic solution (5 mM NaCl) and incubated on ice for 15 min to allow the cells to swell. Cells were subsequently lysed by adding a cell lysis buffer (10 mM NaCl, 5 mM $MgCl_2$, and 0.33% NP-40) to release nuclei from the cytoplasm. Purity and integrity of the nuclei were confirmed under light microscope.

DOI: 10.1002/jgm

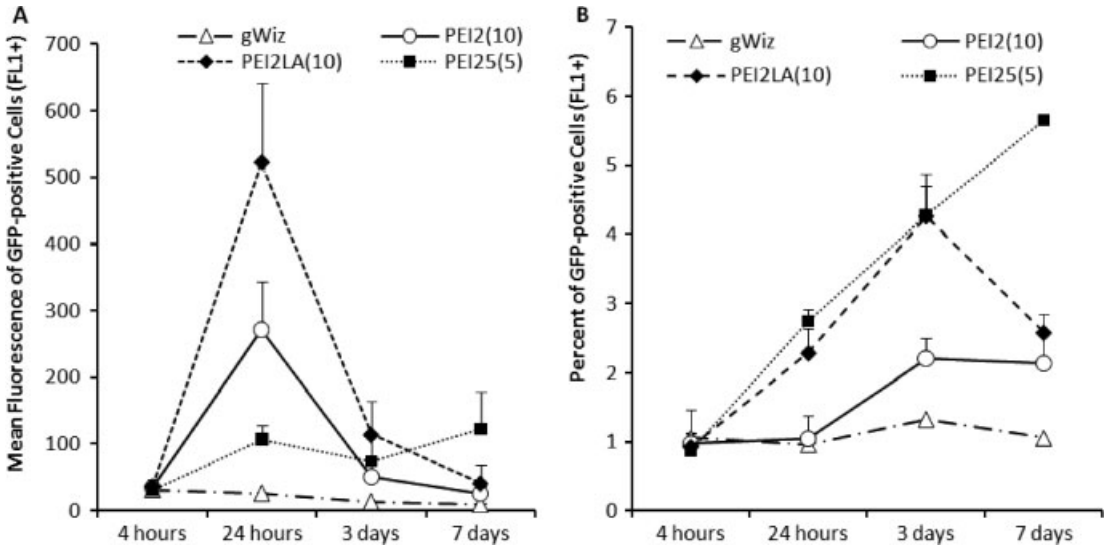

Figure 1. Transfection efficiency with PEI2, PEI2LA and PEI25 polyplexes in rBMSC as collectively represented by (A) the mean fluorescence of GFP-positive cells and (B) the percentage of transfected cells (FL1+) over a 7-day experimental period. Analysis was carried out by calibrating the autofluorescent value against rBMSC treated with gWIZ polyplexes, which had no reporter gene in the expression plasmid. Maximum GFP fluorescence intensity was observed on day 1, although the percentage of GFP-positive cells was gradually increased over the study period

CLSM and image quantification

Rat BMSC were seeded onto a number 1 1/2 glass coverslip measuring 18 × 18 mm (Fischer Scientific, Pittsburgh, PA, USA) in six-well plates and transfected as described above. At designated time point, cells were fixed in 3.7% formalin in HBSS for 15 min and washed with HBSS. 12-bit images were acquired using an inverted Zeiss LSM 710 Laser Scanning Confocal Microscope (Carl Zeiss, Oberkochen, Germany) through a 1.3 NA 40 × Plan-Fluar oil-immersion objective with a field view of 103.7 × 103.7 nm/pixel. Cy5-labeled pDNA was excited by the 5 mW HeNe-laser (633 nm); GFP was excited by the 25 mW Ar-laser (488 nm). Nuclei were stained with Hoechst 33 528 (300 ng/ml) for 15 min and excited by the 405 nm laser. Quantification of images acquired by CLSM were performed using NIH ImageJ (http://rsbweb.nih.gov/ij/) with a collection of plugins for microscopy analysis downloaded from the McMaster Biphotonics Facility (MBF_ImageJ, http://www.macbiophotonics.ca/). The stained nuclei were used to define the region of interest to derive fluorescent intensity values from the Cy5 channel and used to calculate the percentage of nuclei with pDNA associated as well as the distribution of pDNA, after a threshold value was defined to take into account autofluorescence and background noise from the images.

Statistical analysis

Where indicated, the data is summarized as the mean ± SD of triplicate measurements. Unpaired Student's *t*-test was used to assess statistical differences ($p < 0.05$) between the group means.

Results

Polyplex sizes in transfection medium

The hydrodynamic sizes of the polyplexes were measured to determine any functional relationship between particles sizes and the level of transgene expression. Measurements were taken in conditions that were representative of those carried out in transfection. That is, complexes were first prepared in 150 mM NaCl and then subsequently diluted in OptiMEM supplemented with 1% FBS at 37 °C to give the same final DNA concentration as those applied in tissue culture. In the absence of complexes, OptiMEM + 1% FBS gave two peaks in the intensity histogram at mean sizes 60 and 10 nm (see Supporting information, Figure 1A). No stable measurements can be taken with OptiMEM only, and hence, these two peaks were likely a result of serum protein from FBS. When polyplexes were added to the media, three peaks were observed in the intensity histogram (see Supporting information, Figure 1B). Two of the peaks are below 100 nm, similar to the sizes of the two peaks observed in OptiMEM 1% FBS only and thus were presumed to be the serum protein. The additional third peak had a much larger size distribution (>200 nm) and is taken as the peak corresponding to the polyplexes. We noted that the peaks corresponding to the serum protein shifted in sizes in the presence of polyplexes, depending on the polymer-to-pDNA weight ratios used to prepare the polyplexes. This suggests that interaction between proteins in the serum and the polyplexes may take place in the media, altering the overall sizes of the polyplexes during transfection.

Complexes were prepared at different polymer-to-pDNA weight ratios by adjusting either the concentration

DOI: 10.1002/jgm

Table 1. The particle size (Z_{ave}, nm) and polydispersity index (PdI) of polyplexes prepared for the present study

Polymer-to	PEI25		PEI2LA		PEI2	
pDNA ratio (w/w)	2 μg/ml pDNA	1 μg/ml pDNA	2 μg/ml pDNA	1 μg/ml pDNA	2 μg/ml pDNA	1 μg/ml pDNA
1.3	662.5 (0.547)	1099 (0.689)				
2.5	228.8 (0.661)	389.8 (0.386)	401.9 (0.401)	3048 (1.000)	1671 (0.853)	3964 (1.000)
5	210.3 (0.551)	146.2 (0.520)	867 (0.689)	1115 (0.684)	1325 (0.826)	1211 (0.717)
10			834.4 (0.685)	634.4 (0.572)	947.0 (0.617)	626.3 (0.555)

Data are shown as the average value of 12 runs, where the number in parenthesis indicates the PdI. The complexes were prepared at polymer-to-pDNA weight ratios of 2.5, 5 and 10, and at pDNA concentrations of 1 and 2 mg/ml. In general, the sizes of the particles were inversely correlated with polymer-to-pDNA weight ratio; the sizes were proportional to the concentration of pDNA.

of pDNA or the concentration of the polymers. The hydrodynamic sizes of the resulting polyplexes are summarized in Table 1. The particle sizes for PEI2LA (10) were not significantly different from PEI2 (10) at the weight ratio used for transfection. Polyplexes of PEI25 (5) were, however, approximately four times smaller than polyplexes of PEI2LA (10) and PEI2 (10) (210 mm versus 947 nm and 834 nm, respectively). The same size differences were observed when the amount of pDNA was reduced, while maintaining the same relative polymer-to-pDNA weight ratio, where PEI25 polyplexes particles were again approximately four times smaller than PEI2 and PEI2LA particles (146.2 nm versus 626 nm and 634 nm, respectively). Thus, the relative polyplexes sizes between PEI2, PEI2LA and PEI25 did not appear to be affected by the concentrations of the polymers or the pDNA. When the concentration of pDNA was reduced, the particle sizes were comparatively smaller, suggesting that the size of the polyplexes may reflect the amount of pDNA packed per particle. This trend was only observed at the highest weight ratios tested. At lower ratios, polyplexes tended to form clusters of aggregates that ranged in sizes with varying degree of aggregation. The aggregation would affect accurate calculation of individual particles sizes and may account for the lack of correlation between particle sizes and pDNA concentrations at the lower weight ratios. Increasing the polymer:pDNA ratio, however, generally reduced the particle sizes for all complexes, indicating a stabilizing effect of the excess polymer on particle sizes.

Correlation between pDNA uptake and transgene expression

To evaluate the relationship between pDNA uptake and transgene expression, multiplexed flow cytometry were carried out to measure the amount of Cy5-labeled pDNA internalized by the cell and the subsequent GFP fluorescence expressed. To compare the efficacy among PEI2, PEI2LA and PEI25, each polyplex was prepared at the polymer-to-pDNA weight ratio that were previously determined to be the most effective for transfection. The weight ratios used for each polymer are indicated in parenthesis where appropriate.

Transfection efficiency is summarized by the level of transgene expression (Figure 1, mean fluorescence of GFP-positive cells) and the percentage of transfected cell (percentage of GFP-positive cells). The highest level of transgene expression was observed 24 h after polyplexes were applied to the cell (Figure 1A). The highest percentage of transfected cells was observed on day 3 for PEI2 and PEI2LA and on day 7 for PEI25 (Figure 1B). The levels of transgene expression from PEI2LA and PEI2 transfected rBMSC were significantly higher than PEI25 ($p < 0.05$). PEI25 and PEI2LA were able to transfect significantly higher percentages of cells than PEI2.

The amount of pDNA uptake for each carrier is summarized in Figure 2A. The mean fluorescence of Cy5-positive cells declined over the one-week experimental period. The drop in pDNA content may be a result of cell division, decrease in fluorescent intensity over the flourophore half-life time and/or pDNA degradation by intracellular nucleases. There was no significant difference in the amount of pDNA uptake between PEI2 and PEI2LA or between PEI2 and PEI25. By day 3, the amount of pDNA in cells was approximately two-fold lower with PEI2LA complexes compared to PEI2 and PEI25 (2.2-fold and 2.1-fold, respectively). The percentage of cells with pDNA uptake were greater than 90% for all carriers from day 1 to day 3 and showed no significant difference between carriers (data not shown).

The relationship between the level of transgene expression and the amount of pDNA internalized on day 1 is shown in Figure 2B. An r^2 value of 0.0101 was obtained, suggesting there was no correlation between GFP expression and pDNA uptake at this time point. We did not perform the analysis for the other time points because the mean GFP fluorescence declined after day 1 to background levels, which might be associated with large errors. A correlation between the GFP fluorescence and pDNA uptake at the single cell level was also analyzed based on a scatter plot of fluorescent intensity from the FL1 (GFP expression) and FL4 (pDNA uptake). Representative plots for each of the carrier are shown in the Supporting information (Figure S2). All GFP-expressing cells had pDNA uptake and were found in the top-right quandrant of the two-dimensional plot. However, there was no apparent relationship between the intensity of GFP fluorescence and the amount of Cy5-labeled pDNA uptake. This further suggests that, although DNA uptake is a prerequisite for transfection, the amount of DNA uptake was not correlated with the level of transgene expression.

DOI: 10.1002/jgm

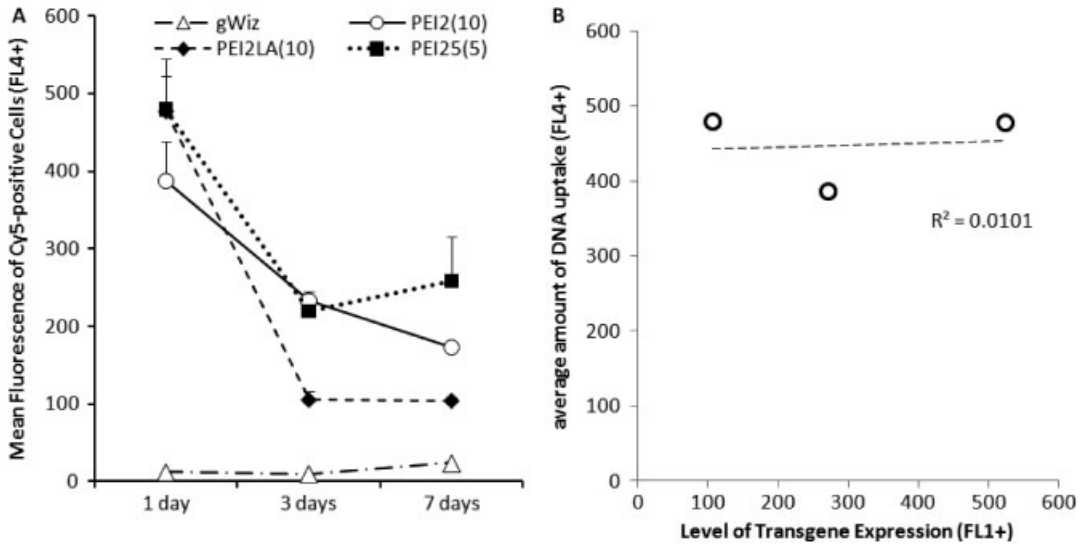

Figure 2. The amount of cellular uptake of Cy5-fluorophore labeled pDNA polyplexes in rBMSC on days 1, 3 and 7. (A) The amount of pDNA uptake in Cy5-positive cells (FL4+) and (B) the correlation between the amount of pDNA (FL4 +) and the level of transgene expression (FL1+) on day 1. There was a gradual reduction of pDNA from day 1 and a lack of correlation between the pDNA uptake and GFP expression

Nuclear-associated pDNA and transgene expression

The conditions used to release nuclei from whole cells were optimized to obtain intact nuclei that were free of cytoplasmic debris, as visually inspected under a phase contrast microscope, and robust enough to be analyzed with a flow cytometer. The rBMSC were on average significantly larger in size compared to typical cultured cell lines such as HEK 293T (19 versus 13 μm). The relatively higher volume ratio of cytoplasm-to-nuclei makes purifying nuclei technically challenging. We employed a hypertonic shock treatment before cell lysis to loosen and dilute the cytoplasm, followed by treatment with low concentration of non-ionic detergent in the presence of a divalent cation. A typical nucleus released into suspension using this protocol is shown in the supporting information (Figure S3). Although this treatment worked to significantly improve the purity of nuclei, a small percentage of nuclei might still have had cytoplasmic debris associated. Additional measures to counter these contaminants were performed through selective gating following FACS. Nuclei associated with cytoplasmic debris were presumably larger than free nuclei, which would translate into a rightward shift on the forward scatter histogram (FSC-H). A typical scatter plot for nuclei is shown in the Supporting information (Figure S4). Free nuclei produced a distinct population concentrated around the lower end of the FSC, enabling the larger cytoplasm associated contaminating nuclei to be excluded from the gated population.

To evaluate the correlation between nuclear-associated pDNA and transgene expression, a portion of the cells used for multiplexed flow cytometry described above were processed for nuclei extraction. The amount of pDNA associated with nucleus is summarized in Figure 3A. In general, nuclear-associated pDNA declined rapidly over a one week period and was near background level by day 7. The amount of pDNA associated with the nucleus was highest in PEI2LA polyplexes at 24 h and was significantly greater than either PEI2 or PEI25 polypolexes ($p < 0.05$).

The relationship between the amount of nuclear-associated pDNA and the level of transgene expression was show in Figure 3B. An r^2 value of 0.8362 was obtained, suggesting a high correlation between the two parameters.

CLSM image quantification of nuclear-associated plasmid DNA

To further support the data obtained from flow cytometry, we examined the nuclear association of pDNA using CLSM. Representative images of the subcellular distribution of the polyplexes relative to nuclei are shown in Figure 4. With PEI25 polyplexes, the particles were relatively small and densely distributed throughout the cell; many of the particles could be seen in and around the nuclear periphery and inside the nucleus (Figure 4A). By contrast, PEI2 polyplexes displayed aggregate-like pDNA clusters with only a few large particles sparsely distributed in the cytosol (Figure 4B). PEI2LA polyplexes exhibited similar clustered such as pDNA aggregates as PEI2 polyplexes; however, the morphology of the fluorescent particles had a bundled filamentous appearance (Figure 4C). The relative sizes of the particles were consistent with the particle sizes obtained from the photon correlation spectroscopy.

To systematically evaluate the extent of nuclear uptake of pDNA, images acquired from random regions on the glass slide were quantified for percentage of nuclei positive for pDNA and the amount of pDNA associated to

DOI: 10.1002/jgm

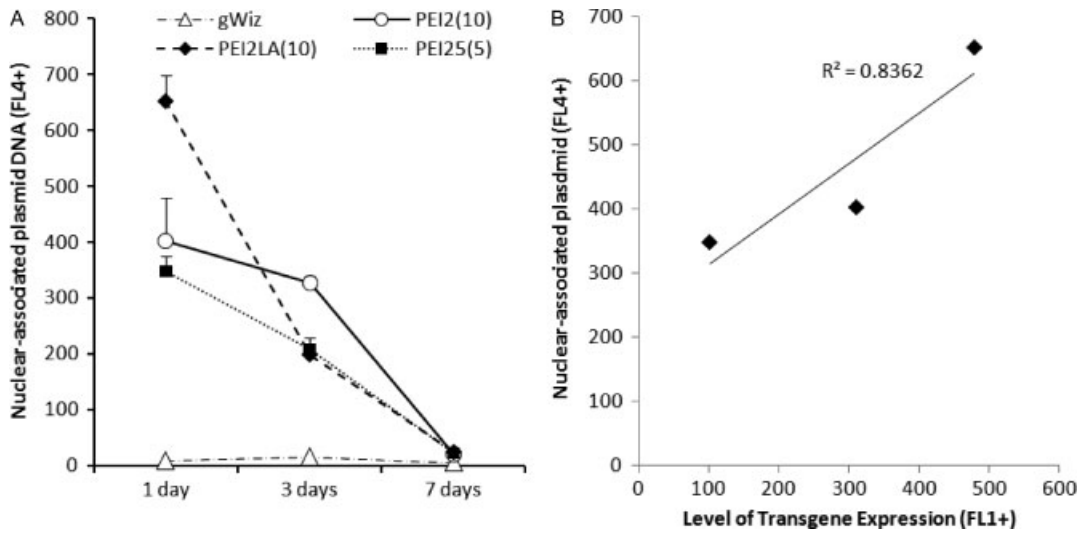

Figure 3. (A) The amount of nuclear-associated Cy5-fluorophore labeled pDNA in rBMSC at days 1, 3 and 7 and (B) the correlation between the amount of nuclear-associated pDNA (FL4+) and level of transgene expression (FL1+) on day 1. Similar to cellular uptake (Figure 2A), there was a gradual reduction in nuclear associated pDNA but a good correlation between the nuclear accosiated pDNA and the GFP expression

each positive nucleus. The number of cells sampled for quantification was in the range 40–55. The percentage of nuclei with pDNA association (pDNA + nuclei) is summarized in Figure 5 for two incubation periods (4 and 24 h). Both PEI2LA and PEI25 treated cells had significantly higher percentage of nuclei with pDNA associated compared to PEI2 at 4 h (89%, 85% and 51%, respectively). The amount of pDNA associated with each nucleus for each polymer was further calculated and tabulated into a box plot histogram (Figure 6). At 4 h, the average fluorescent intensity of PEI25 polyplexed pDNA clusters was 61.9, which was significantly lower than PEI2 and PEI2LA, each with an average intensity value of 92.5 and 148.0, respectively. A similar trend was observed at 24 h as well, where the average fluorescent intensity of PEI25 polyplexed pDNA was lower than both PEI2 and PEI2LA (75.8 versus 116.9 and 184.5, respectively). In terms of distribution, PEI25 had an approximately symmetrical interquartile range with a median of 58.4 at 4 h, whereas both PEI2 and PEI2LA had larger inter-quartile region with median values of 62.6 and 105.3, respectively, and displayed positively skewed distributions. For PEI25, the third quartile fell in the range 58.8–70.9, a much lower and narrower range than PEI2LA, which ranges from 105.3–203.1. At 24 h, a similar trend continued but the interquartile range for each polymer was narrower than at 4 h. PEI2LA still has the highest mean value (186.3) follow by PEI2 (117.3), with the lowest being PEI25 (75.9). Taken together, these data showed that, although PEI25 polyplexes were able to associate with more nuclei than PEI2, each nucleus had low amounts of pDNA associated. The majority of nuclei associated with PEI2LA polyplexes had a significantly greater amount of pDNA than PEI25 polyplexes.

Subcellular distribution of pDNA in GFP positive and negative cells

Using the Cy5-labeled pDNA, we were able to perform multiplexed confocal microscopy to visualize both GFP expression and pDNA localization simultaneously. Using this dual labeled technique, we aimed to determine whether there was a difference in the nuclear distribution of pDNA between GFP positive cells (GFP+) and GFP-negative (GFP−) cells. Representative confocal images of GFP-expressing cells on day 1 from the regions sampled are shown in Figure 7. Similar to particles observed on day 1, PEI25 polyplexes were smaller and more uniformly distributed throughout the cell (Figure 7A) than PEI2LA, whose polyplexed pDNA clusters were aggregated, string-like and punctate in distribution (Figure 7B). The number of cells sampled for quantification was in the range 34–61 for PEI2LA and PEI25. It had been demonstrated elsewhere that 30 cells are sufficient to draw a general conclusion from the statistical point of view [21]. However, we were not able to perform a statistically significant distribution comparison for PEI2 because there were insufficient transfected cells. The fluorescent intensity distribution box plot histrogram for PEI25 and PEI2LA are shown in Figure 8. In general, the distributions of nuclear-associated pDNA in GFP+ cells were positively skewed and had a much larger range than GFP− cells. Further, in both polymers, the mean fluorescence values of the GFP+ distributions were higher than GFP− (marked bold lines in each box plot). These data suggest that the majority of the GFP+ cells had higher pDNA associated with their nuclei compared to GFP− cells.

DOI: 10.1002/jgm

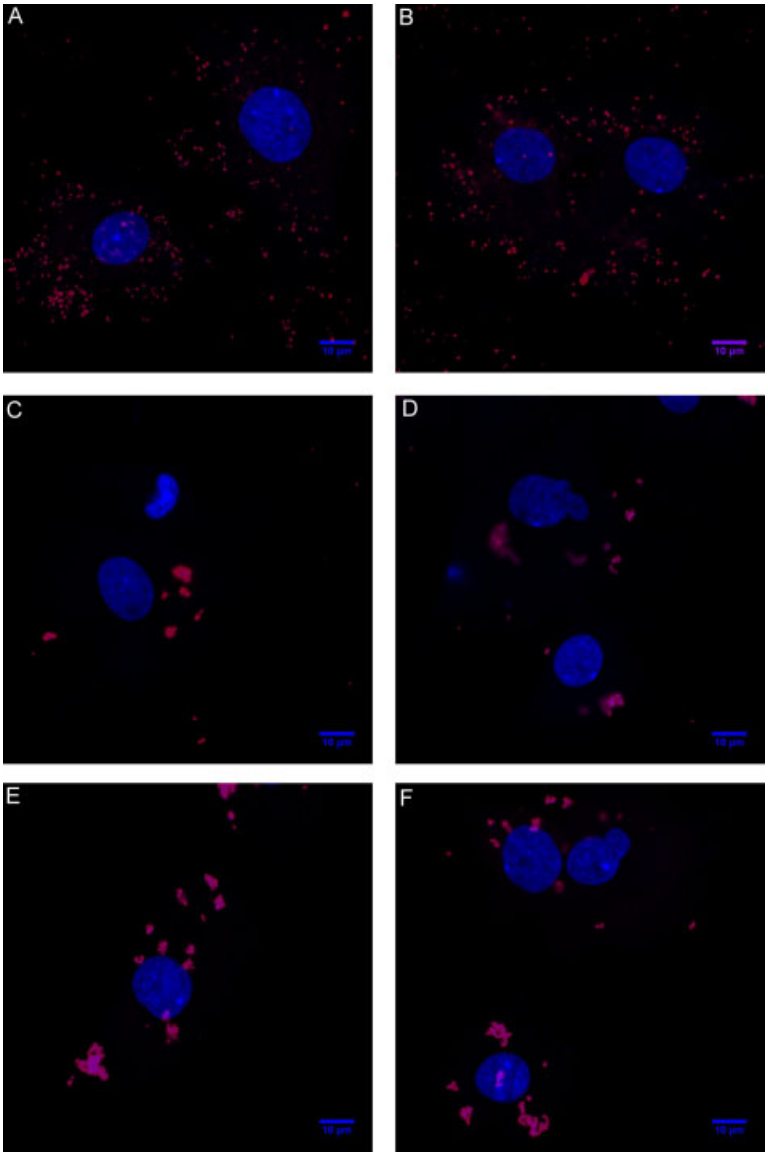

Figure 4. CLSM showing typical images of rBMSC nuclear-associated pDNA at 4 h after incubation with polyplexes of (A) PEI25 (B) PEI2 and (C) PEI2LA. Nuclei are stained with Hoechst 33258. Post image processing was applied to display the nuclei in blue and Cy5-labeled pDNA clusters in red–purple. Note the dispersed distribution of PEI25 polyplexes, unlike the clustered distribution of PEI2 and PEI2LA polyplexes (scale bar = 10 μm)

Discussion

We previously demonstrated that the ineffective cationic polymeric gene carrier PEI2 can be modified into an effective transfection agent through lipid substitution with linoleic acid [12]. In the present study, we provided a mechanistic look at the intracellular kinetics of the lipid modified polyplexes with respect to trafficking to the nuclear periphery. We employed a dual modality approach using a combination of high-throughput flow cytometry and CLSM to characterize the intracellular trafficking of polyplexes. A key aspect of this approach was the multiplexed fluorescent labeling, which allowed us to quantitatively correlate pDNA with transgene expression directly. We demonstrated that improved transfection efficiency seen in PEI2LA was a result of enhanced trafficking and association with the nuclear periphery, which is considered to reflect nuclear uptake of the transgene during the transient breakdown of nuclear envelope in mitosis. Furthermore, transgene expression was correlated with nuclear-associated pDNA, and not cellular pDNA uptake, consistent with findings reported previously for other nonviral gene carriers in the immortalized HeLa cells [18,22]. The differences in the level of transgene expression between PEI2LA and PEI25 appeared to be correlated with the size of the polyplexes, which may reflect the amount of pDNA packed per particle, and thus the amount of template available for expression. The distribution in the fluorescent intensity of pDNA associated nuclei among GFP-expressing transfected cells was positively skewed with a concurrent rightward shift towards higher average than those apparent non-expressing or

DOI: 10.1002/jgm

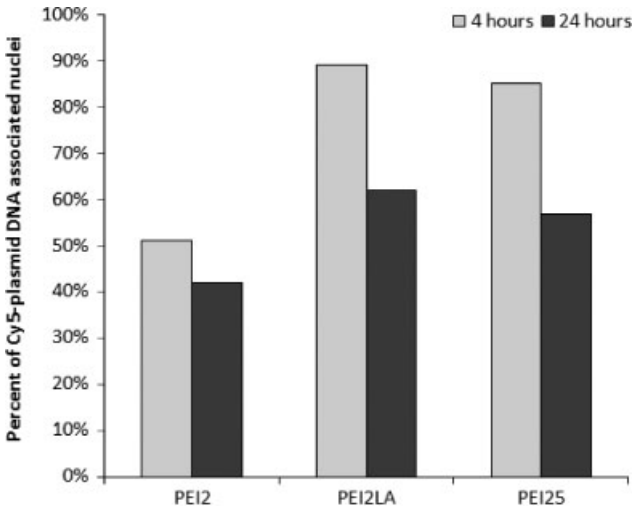

Figure 5. Percentage of nuclei with pDNA associated at 4 and 24 h after initial incubation with the PEI2, PEI2LA or PEI25 polyplexes as quantified by image analysis. Images were optically sliced using CLSM to obtain the section with the thickest nuclei density. pDNA-positive nuclei were identified by defining the nucleus as the region of interest (ROI); nuclei which had a fluorescent value above the arbitrary defined background was scored as positive ($n = 34–66$). Note the better nuclear association of pDNA as a result of delivery with PEI25 and PEI2LA

low expressing cells, suggesting a transgene expression dependency on template copy number.

Post-translational modifications of endogenous proteins are crucial for protein trafficking to various sub-cellular compartments. Lipid modification is one of the strategies employed by the cell to provide additional functional and regulatory control beyond genomic information to maintain intracellular homeostasis. For example, proteins modified with the lipid palmitate allow targeting to specialized membrane microdomains involved in synaptic scaffolding, signaling and cytoskeletal proteins [23]. Palmitoylation may act as a replacement for membrane spanning protein domains by serving as the interface to the hydrocarbon core of the lipid bilayer. Thus, lipid moieties may act as a membrane anchor to enhance the hydrophobicity of proteins and contribute to their membrane association [24]. In a similar fashion to the lipid-modified proteins, lipid-modified cationic polymers may facilitate association of polyplexes to various membrane bound subcellular compartments, including the nucleus. Indeed, we have observed an increase in the amount of nuclear-associated pDNA with PEI2LA complexes compared to its unmodified parental molecules, PEI2. However, it is reasonable to infer that the hydrophobic interaction is a nonspecific event and that the positively charged polyplexes may also interact with other negatively charged lipid moieties on other membrane-bound organelles such as the endoplasmic reticulum, golgi complex and mitochondria [25]. Therefore, the nuclear association of the polyplexes may be limited by nonspecific binding to other intracellular compartments. This issue needs to be further explored and, if found to be significant, strategies to improve specific binding of polyplexes with the nuclear membrane may further increase transfection efficiency.

It is generally held that the strong correlation between nuclear associated pDNA and transfection efficiency is a result of the spatial proximity of the transgene to the nucleoplasm, which increases the probability of pDNA nuclear translocation during mitosis. That is, during prophase when the nuclear envelope is transiently broken down, the absence of the physical barrier grants pDNA access to nucleoplasm for it to bind to chromatin and/or nuclear proteins. This allows pDNA to be tethered onto nuclear materials and be incorporated into the nucleus following telophase, when the nuclear envelope reassembles. However, recent evidence suggests that the breakdown of nuclear envelope may not be necessary for nuclear translocation. Kamiya *et al*. [26] investigated the nuclear uptake of lipoplexes in the presence of intact nuclear membrane and observed that some pDNA appeared to extend through the nuclear membrane in the aggregated form, and were much larger than the nuclear pore complex, similar to our observation of PEI2LA polyplexes in CLSM. The authors reasoned that lipoplexes fused with the nuclear membrane and the electrostatic interaction between the complex and the membrane led to the release of pDNA into the nucleus [26]. Such a fusion and dissociation event may also take place with lipopolyplexes employed in the present study.

The intensity of GFP fluorescence from cells transfected with low molecular weight PEIs (PEI2LA and PEI2) was consistently higher than those transfected with PEI25, indicative of higher transgene expression activity from the former two carriers. This may be accounted by the differences in the binding affinity to pDNA. The level of transgene expression has been shown to be directly correlated with vector unpacking of DNA; Itaka *et al*. [27] found that the disparity in transfection efficiency between linear PEI and branched PEI was directly correlated with their pDNA dissociation kinetics. Similarly, higher transfection efficiencies seen in low molecular weight polyplexes was attributed to their ability to dissociate and decondense DNA more readily than high molecular weight polyplexes [28–29]. Although we did not observe any difference in the dissociation kinetics between PEI2 and PEI25 previously, we did see a stronger pDNA binding with PEI25 [12] and could explain the lower level of transgene expression observed with PEI25 complexes.

A second explanation for the difference in transgene expression among carriers is the amount of pDNA packed per particle. With both dynamic light scattering (DLS) and CLSM, we observed significantly larger clusters of pDNA in low molecular weight PEI polyplexes compared to PEI25 polyplexes. Because the pDNA used in the present study was covalently labeled with a fluorophore, the intensity of the fluorescence was presumed to be proportional to the amount of pDNA present. The observation that PEI2 and PEI2LA complexes had larger pDNA clusters suggests that there are more molecules of pDNA per cluster. The relationship between particle size and pDNA content was also verified under DLS; at a given polymer-to-pDNA weight ratio, when the pDNA concentration was reduced, the

DOI: 10.1002/jgm

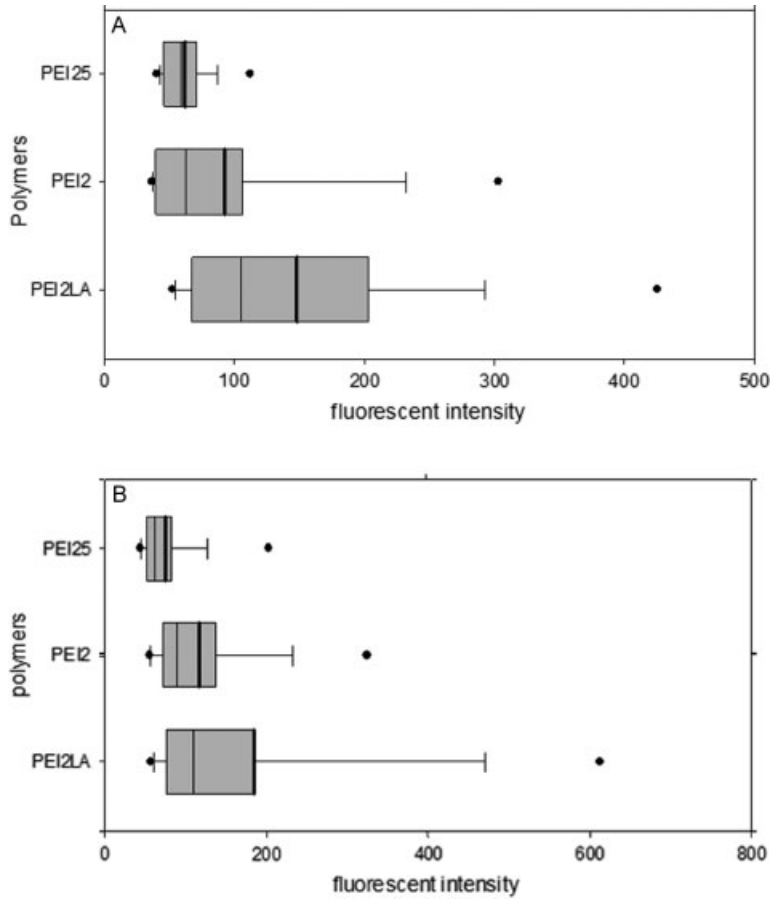

Figure 6. Box plot histogram distribution in fluorescent intensity of pDNA associated with nuclei from rBMSC at 4 h (A) and 24 h (B) after initial exposure with polyplexes of PEI2, PEI2LA and PEI25. The data were derived by quantitating images acquired by CLSM. Grey shaded boxes represent the middle 50% of the data range, and the thick solid line in the box denotes the mean fluorescent value; black solid circle-dots denote the minimum and maximum values and define the range. Note that PEI2LA had the highest mean value and the largest range, whereas PEI25 had the lowest mean and the smallest range at both 4 h and 24 h

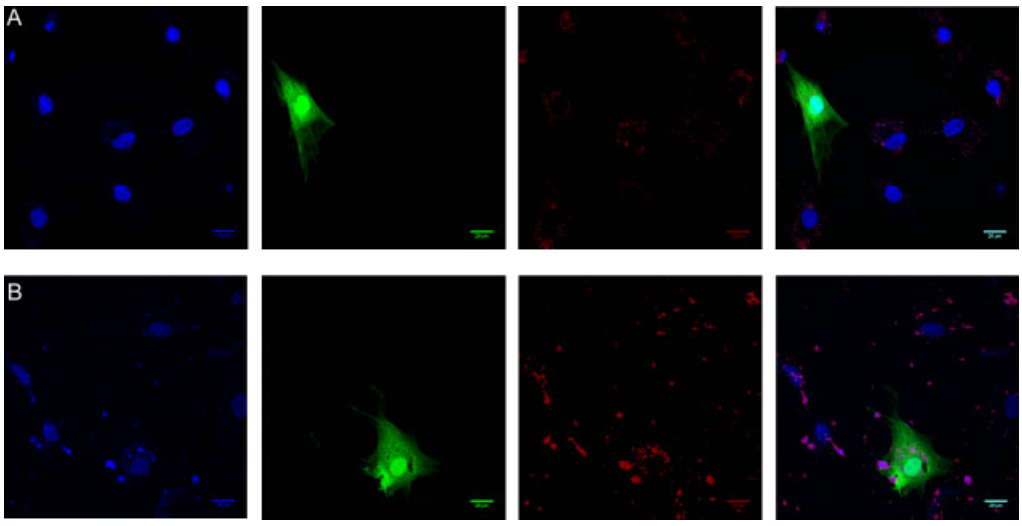

Figure 7. Representative CLSM images of GFP-positive (GFP+) cells transected with (A) PEI25 and (B) PEI2LA. Nuclei were stained with Hoescht 33258 and the pDNA were labeled with Cy5. Post image processing was performed to show the nuclei in blue (left column), GFP in green (second column from left) and pDNA cluster in red (third column from left). Composite images are shown on the right column. (scale bar = 20 μm). Note the dispersed PEI25 polyplexes in contrast to the aggregated, cluster-like appearance of PEI2LA polyplexes

DOI: 10.1002/jgm

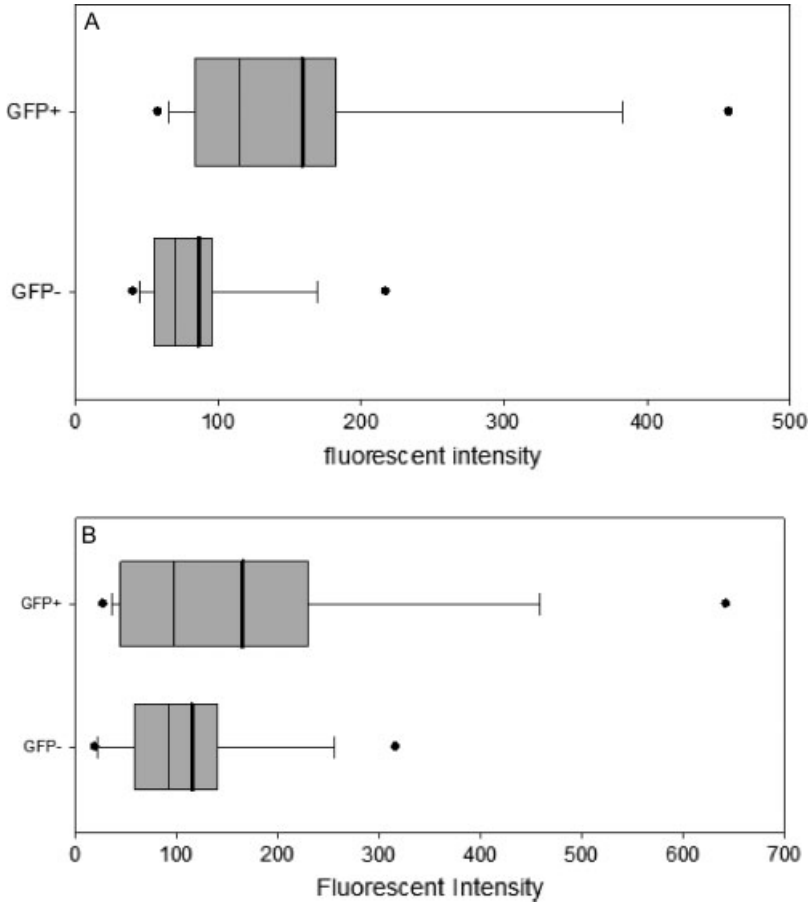

Figure 8. Box plot histogram distribution in fluorescent intensity of pDNA associated with nuclei between transfected cells (GFP+) and nontransfected cells (GFP−) at 24 h after exposure to polyplexes of (A) PEI25 and (B) PEI2LA. Grey shaded boxes represent the middle 50% of the data range and the thick solid line in the box denotes the mean fluorescent value; black solid circle-dots represent the minimum and maximum values, which together define the range of the distribution. Note in both PEI25 and PEI2LA, the GFP+ population had greater mean values and a larger range than GFP−. In addition, the GFP+ distribution was positively skewed

hydrodynamic sizes of the complexes became smaller, suggesting fewer pDNA molecules were packed per polyplex on average. Thus, the higher level of transgene expression seen in low molecular PEIs may be a result of more copies of pDNA packed per particle available for transgene expression than PEI25 with smaller, fewer templates.

A third explanation supplementary to the pDNA cluster size is the distribution in the amount of pDNA associated with each nucleus. Nuclei from cells treated with PEI25 polyplexes had much lower fluorescent intensity than either PEI2 or PEI2LA. Indeed, even though PEI2LA and PEI25 treated cells had approximately same percentage of nuclei with plasmid DNA, the intensity of fluorescently labeled pDNA was much higher with PEI2LA. In other words, there was more pDNA associated with each nucleus from cells treated with PEI2LA polyplexes than PEI25. This suggests that more pDNA is available for subsequent nuclear translocation and transgene expression, leading to higher transfection efficiency.

We further examined the nuclear association of pDNA between GFP+ and GFP− cells to determine whether the heterogeneity in transgene expression is attributed to the amount of pDNA associated with the nucleus. We found with both PEI2LA and PEI25 polyplexes that GFP+ cells had higher amounts of pDNA associated with the nuclei than those non-expressing ones. On a population scale, this is consistent with previous studies [18,30] and supports the data derived from flow cytometry indicating that nuclear-association is correlated with transgene expression. However, at the single cell level, the nuclear pDNA distributions does not explain why some cells with apparent low pDNA/nuclear association express GFP, whereas some with high pDNA association show no transgene expression. This further highlights the intrinsic cell-to-cell differences that appear to be of greater importance than the intracellular trafficking and physical interaction of polyplexes. The heterogeneity in transgene expression may be a result of the cells being in different cell cycle stages. Many reports have demonstrated that cells undergoing the S- to M-phase of the cell cycle tend to exhibit enhancement in transgene expression [14–17]. Given that approximately 20% of the cells in the population were likely to be in the G2/M, and that the percentage of nuclei with plasmid associated had dropped to 50–60% by day 1, this leaves only approximately 10–12% of the cells primed for transgene expression.

DOI: 10.1002/jgm

Presumably, the dependency on the M-phase is a result of the breakdown of the nuclear membrane and entry of the transgene into the nucleus. However, a recent study has shown that the heterogeneity and cell cycle dependency may be attributed to the events associated with the S- and M-phases [31]. During the S-phase, histones are actively synthesized to prepare for the daughter genome following mitosis. The increase in intranuclear concentration of histone may induce decondensation of polyplexes by competitive dissociation and may even form a nucleosome structure with the pDNA, which is primed for efficient transcription. In addition, following decondensation, the released polymeric gene carrier may continue to interact with other nucleic acids, even the newly-synthesized transgene mRNA, thereby inhibiting the translation [32]. Thus, transgene expression efficiency may involve a dynamic equilibrium between the gene carrier, pDNA and nuclear materials, which is closely associated with the homeostasis of the cell. Irrespecitve of the specific factors, intranuclear trafficking appears to play a vital role in determing transgene expression. Pharmacokinetics studies of nonviral gene carriers have so far being limited to cytoplasmic trafficking; with no emphasis on the fate of polyplexes in various subnuclear domains. Investigation into intranuclear trafficking of nonviral pDNA polyplexes may provide significant insight on barriers to transfection.

The eventual goal following on from the present study is to develop a BMSC-based therapy for bone regeneration by directing osteogenic differentiation *in vitro* using nonviral gene carriers as a transfection agent and subsequently transplanting the modified cells back to the patient. Intracellular mechanistic studies and carrier optimization of nonviral gene carrier are often performed in transformed immortalized cell line such as HEK293T, HeLa and COS-7 cells with the aim that information derived will be applicable to a clinical model. However, data derived in this setting are limited in clinical relevance because (i) immortalized cell lines cannot be used for clinical application as a result of tumorigenicity concerns and (ii) transfection efficiency varies greatly between cell types (a transfection agent effective in one type may not be effective at all in another and the relative efficiency between carriers appears to lack concordance in this regard) [18,33–35]. This difference seemed to arise as a result of cellular physiology, which affects the uptake and intracellular trafficking pathway. For example, a recombinant Ad5 penton based protein, which has been incorporated as molecular conjugates for its cell binding and endosomolytic activity, was reportedly internalized efficiently by HeLa cells [36,37] but remained on the surface of primary acinar epithelial cells even after prolonged incubation, with no evidence of internalization [38]. More importantly, transformed cell lines are 'too' easily transfected, indicating that the relevant biological barriers present in patient cells have been removed in transformed cells. Thus, mechanistic studies are ideally conducted in the primary cell type that is ultimately going to be used for clinical application such that strategy towards carrier optimization can be directly applied.

In conclusion, the present study demonstrates that enhanced transfection efficiency mediated by lipid substitution of a low molecular weight cationic polymeric gene carrier in rBMSC was a result of increased association of lipophilic polyplexes with the nuclear periphery; association with other membrane-bound structures is a possibility that reduces available pDNA from nuclear uptake and should be investigated further. GFP-positive cells had, on average, a greater amount of pDNA associated with their nuclei than GFP-negative cells, reinforcing the notion that trafficking to the nucleus is critical for transfection. However, nuclear uptake alone cannot predict transfection at the individual cell level because cells that display high pDNA nuclear disposition did not always express GFP. This suggests that intranuclear trafficking and intranuclear factors may play a further role in determining the outcome of transfection.

Acknowledgements

We are grateful to Dr. Vanessa Incani for the preparation of PEI2LA and Mr Cezary Kucharski for the tissue culture work. This project is supported by Canadian Institute of Health Research (CIHR), Natural Sciences and Engineering Research Council (NSERC) of Canada and Alberta Advanced Education and Technology. Equipment support from the Alberta Heritage Foundation for Medical Research (AHFMR) is greatly appreciated. Mr C.Y.M. Hsu is financially supported by the NSERC Alexander Graham Bell Canada Graduate Scholarships. We also thank Geraldine Barron (Alberta Health Services) and Dr Xuejun Sun (Department of Experimental Oncology) for their assistance with confocal microscopy. The authors report no conflicts of interest. The authors alone are responsible for the content and writing of the paper.

Supporting information

Figure S1. Typical intensity histogram of particle sizes. (A) OptiMEM with 1% FBS with no particles. (B) PEI25/pDNA polyplex at polymer-to-pDNA weight ratio of 2.5 at a pDNA concentration of 2 μg/ml, in OptiMEM + 1% FBS. Note the third peak with the highest intensity and a mean size of 210 nm. This peak was not present in the previous figure and is taken as the peak corresponding to the PEI25 polyplexes.

Figure S2. Two-dimensional histogram plotted with fluorescent intensity values from the FL1-H (GFP) and FL4-H (Cy5-labeled pDNA) channels of rBMSC treated with polyplexes of (A) PEI2 (B) PEI2LA and (C) PEI25 as measured by flow cytometry. The horizontal-vertical perpendicular lines in the graph divides cells into populations, which represents cells with no pDNA uptake and no GFPexpression (bottom left), cells with GFP-expression but no pDNA uptake (bottom right), cells with pDNA uptake but no GFP-expression (top left) and cells with pDNA uptake and GFP-expression (top right). Note the scatter distribution of dots in the top right quandrant, which indicates no strong correlation between GFP fluorescence and pDNA uptake.

Figure S3. Representative images of isolated intact nuclei from rBMSC viewed under a phase contrast microscope.

Figure S4. Typical FSC-H and side scatter (SSC) flow cytometric analysis of intact nuclei from rBMSC treated with PEI2LA complexes; cells were treated with 0.33% NP-40 to release nuclei from the cell. (A) raw nuclei scatter. The dense black dot region represents the majority of the nuclei, whereas orange dots near the border lines represent nuclei with cytoplasmic debris contamination. (B) R2 (in green) shows the gate applied to final analysis of pDNA-associated nuclei. In general, singlet of intact nuclei had similar SSC and FSC profile and was found concentric in the lower left region of the graph. By contrast, multiplets and contaminated nuclei were irregular in shapes and sizes and were found scattered near the borders of the graph.

References

1. Thomas CE, Ehrhardt A, Kay MA. Progress and problems with the use of viral vectors for gene therapy. *Nat Rev Genet* 2003; **4:** 346–358.
2. Lungwitz U, Breunig M, Blunk T, *et al*. Polyethylenimine-based non-viral gene delivery systems. *Eur J Pharm Biopharm* 2005; **60:** 247–266.
3. Kakudo T, Chaki S, Futaki S, *et al*. Transferrin-modified liposomes equipped with a pH-sensitive fusogenic peptide: an artificial viral-like delivery system. *Biochemistry* 2004; **43:** 5618–5628.
4. Hyndman L, Lemoine JL, Huang L, *et al*. HIV-1 Tat protein transduction domain peptide facilitates gene transfer in combination with cationic liposomes. *J Control Release* 2004; **99:** 435–444.
5. Kunath K, Merdan T, Hegener O, *et al*. Integrin targeting using RGD-PEI conjugates for in vitro gene transfer. *J Gene Med* 2003; **5:** 588–599.
6. Opanasopit P, Rojanarata T, Apirakaramwong A, *et al*. Nuclear localization signal peptides enhance transfection efficiency of chitosan/DNA complexes. *Int J Pharm* 2009; **382:** 291–295.
7. Yamada Y, Nomura T, Harashima H, *et al*. Intranuclear DNA release is a determinant of transfection activity for a non-viral vector: biocleavable polyrotaxane as a supramolecularly dissociative condenser for efficient intranuclear DNA release. *Biol Pharm Bull* 2010; **33:** 1218–1222.
8. Jeong JH, Kim SH, Christensen LV, *et al*. Reducible poly(amido ethylenimine)-based gene delivery system for improved nucleus trafficking of plasmid DNA. *Bioconjug Chem* 2010; **21:** 296–301.
9. Chen TH, Bae Y, Furgeson DY. Intelligent biosynthetic nanobiomaterials (IBNs) for hyperthermic gene delivery. *Pharm Res* 2008; **25:** 683–691.
10. Lee M, Rentz J, Han SO, *et al*. Water-soluble lipopolymer as an efficient carrier for gene delivery to myocardium. *Gene Ther* 2003; **10:** 585–593.
11. Mi Bae Y, Choi H, Lee S, *et al*. Dexamethasone-conjugated low molecular weight polyethylenimine as a nucleus-targeting lipopolymer gene carrier. *Bioconjug Chem* 2007; **18:** 2029–2036.
12. Neamnark A, Suwantong O, Bahadur RK, *et al*. Aliphatic lipid substitution on 2 kDa polyethylenimine improves plasmid delivery and transgene expression. *Mol Pharm* 2009; **6:** 1798–1815.
13. Khalil IA, Kogure K, Akita H, *et al*. Uptake pathways and subsequent intracellular trafficking in nonviral gene delivery. *Pharmacol Rev* 2006; **58:** 32–45.
14. Brunner S, Furtbauer E, Sauer T, *et al*. Overcoming the nuclear barrier: cell cycle independent nonviral gene transfer with linear polyethylenimine or electroporation. *Mol Ther* 2002; **5:** 80–86.
15. Brunner S, Sauer T, Carotta S, *et al*. Cell cycle dependence of gene transfer by lipoplex polyplex and recombinant adenovirus. *Gene Ther* 2000; **7:** 401–407.
16. Mortimer I, Tam P, MacLachlan I, *et al*. Cationic lipid-mediated transfection of cells in culture requires mitotic activity. *Gene Ther* 1999; **6:** 403–411.
17. Tseng WC, Haselton FR, Giorgio TD. Mitosis enhances transgene expression of plasmid delivered by cationic liposomes. *Biochim Biophys Acta* 1999; **1445:** 53–64.
18. James MB, Giorgio TD. Nuclear-associated plasmid, but not cell-associated plasmid, is correlated with transgene expression in cultured mammalian cells. *Mol Ther* 2000; **1:** 339–346.
19. Clements BA, Hsu CY, Kucharski C, *et al*. Nonviral delivery of basic fibroblast growth factor gene to bone marrow stromal cells. *Clin Orthop Relat Res* 2009; **467:** 3129–3137.
20. Hsu CY, Uludag H. Effects of size and topology of DNA molecules on intracellular delivery with non-viral gene carriers. *BMC Biotechnol* 2008; **8:** 23.
21. Akita H, Ito R, Kamiya H, *et al*. Cell cycle dependent transcription, a determinant factor of heterogeneity in cationic lipid-mediated transgene expression. *J Gene Med* 2007; **9:** 197–207.
22. Glover DJ, Leyton DL, Moseley GW, *et al*. The efficiency of nuclear plasmid DNA delivery is a critical determinant of transgene expression at the single cell level. *J Gene Med* 2010; **12:** 77–85.
23. Fukata Y, Fukata M. Protein palmitoylation in neuronal development and synaptic plasticity. *Nat Rev Neurosci* 2010; **11:** 161–175.
24. Levental I, Grzybek M, Simons K. Greasing their way: lipid modifications determine protein association with membrane rafts. *Biochemistry* 2010; **49:** 6305–6316.
25. Daum G. Lipids of mitochondria. *Biochim Biophys Acta* 1985; **822:** 1–42.
26. Kamiya H, Fujimura Y, Matsuoka I, *et al*. Visualization of intracellular trafficking of exogenous DNA delivered by cationic liposomes. *Biochem Biophys Res Commun* 2002; **298:** 591–597.
27. Itaka K, Harada A, Yamasaki Y, *et al*. In situ single cell observation by fluorescence resonance energy transfer reveals fast intra-cytoplasmic delivery and easy release of plasmid DNA complexed with linear polyethylenimine. *J Gene Med* 2004; **6:** 76–84.
28. Huang M, Fong CW, Khor E, *et al*. Transfection efficiency of chitosan vectors: effect of polymer molecular weight and degree of deacetylation. *J Control Release* 2005; **106:** 391–406.
29. Cho YW, Kim JD, Park K. Polycation gene delivery systems: escape from endosomes to cytosol. *J Pharm Pharmacol* 2003; **55:** 721–734.
30. Bengali Z, Rea JC, Gibly RF, *et al*. Efficacy of immobilized polyplexes and lipoplexes for substrate-mediated gene delivery. *Biotechnol Bioeng* 2009; **102:** 1679–1691.
31. Akita H, Ito R, Kamiya H, *et al*. Cell cycle dependent transcription, a determinant factor of heterogeneity in cationic tipid-mediated transgene expression. *J Gene Med* 2007; **9:** 197–207.
32. Hama S, Akita H, Iida S, *et al*. Quantitative and mechanism-based investigation of post-nuclear delivery events between adenovirus and lipoplex. *Nucleic Acids Res* 2007; **35:** 1533–1543.
33. Douglas KL, Piccirillo CA, Tabrizian M. Effects of alginate inclusion on the vector properties of chitosan-based nanoparticles. *J Control Release* 2006; **115:** 354–361.

34. Dastan T, Turan K. In vitro characterization and delivery of chitosan-DNA microparticles into mammalian cells. *J Pharm Pharm Sci* 2004; **7:** 205–214.
35. Rejman J, Bragonzi A, Conese M. Role of clathrin- and caveolae-mediated endocytosis in gene transfer mediated by lipo- and polyplexes. *Mol Ther* 2005; **12:** 468–474.
36. Medina-Kauwe LK. Endocytosis of adenovirus and adenovirus capsid proteins. *Adv Drug Deliv Rev* 2003; **55:** 1485–1496.
37. Rentsendorj A, Agadjanian H, Chen X, *et al*. The Ad5 fiber mediates nonviral gene transfer in the absence of the whole virus, utilizing a novel cell entry pathway. *Gene Ther* 2005; **12:** 225–237.
38. Hamm-Alvarez SF, Xie J, Wang Y, *et al*. Modulation of secretory functions in epithelia by adenovirus capsid proteins. *J Control Release* 2003; **93:** 129–140.

DOI: 10.1002/jgm